Tetrahedron Letters xxx (2014) xxx–xxx

Contents lists available at ScienceDirect

Tetrahedron Letters

journal homepage: www.elsevier.com/locate/tetlet

Novel 10,13-disubstituted dipyrido[3,2-*a*:2′,3′-*c*]phenazines and their platinum(II) complexes: highly luminescent ICT-type fluorophores based on D–A–D structures

Tatsuya Shigehiro[a], Shigeyuki Yagi[a,*], Takeshi Maeda[a], Hiroyuki Nakazumi[a], Hideki Fujiwara[b], Yoshiaki Sakurai[c]

[a] *Department of Applied Chemistry, Graduate School of Engineering, Osaka Prefecture University, 1-1 Gakuen-cho, Naka-ku, Sakai, Osaka 599-8531, Japan*
[b] *Department of Chemistry, Graduate School of Science, Osaka Prefecture University, 1-1 Gakuen-cho, Naka-ku, Sakai, Osaka 599-8531, Japan*
[c] *Textile and Polymer Section, Technology Research Institute of Osaka Prefecture, 2-7-1 Ayumino, Izumi, Osaka 594-1157, Japan*

ARTICLE INFO

Article history:
Received 12 June 2014
Revised 14 July 2014
Accepted 18 July 2014
Available online xxxx

Keywords:
Dipyridophenazine
Platinum complex
Chromophore
Intramolecular charge transfer
Fluorescence

ABSTRACT

Novel donor–acceptor–donor (D–A–D) π-conjugated molecules based on a dipyrido[3,2-*a*:2′,3′-*c*]phenazine (dppz) skeleton were synthesized, and their luminescent properties were investigated. Introduction of various aryl substituents to the 10- and 13-positions of dppz allowed us to tune the emission properties through modulation of the intramolecular charge transfer (ICT) character on the D–A–D chromophores. Coordination of platinum(II) to the diimine site of dppz also gave rise to facilitation of the ICT to induce a significant red shift of the emission.

Luminescent molecules with organic and organometallic frameworks have so far been developed, aimed at applications in various fields such as biochemical and medicinal analyses,[1,2] chemosensory systems,[3–5] molecular logic gates,[6] organic light-emitting diodes,[7,8] and so on. As traditional fluorescent dyes, coumarines,[9] rohdamines,[10] cyanines,[11] and pyrene derivatives[12] are representative examples, and these dyes are still useful for practical applications. More recently, various types of linearly π-conjugated compounds, including π-conjugated polymers such as poly(phenylene)s,[13] poly(phenylene-vinylene)s,[14] and poly(phenylene-ethynylene)s,[15] have been eagerly developed especially as emitting materials for organic electronics, where critical tuning of HOMO and LUMO levels is necessary to achieve optimized device performance, along with color tuning for their purposes. Intramolecular charge transfer (ICT)-type compounds, consisting of donor (D) and acceptor (A) units, have often been reported, which allows us to tune emission colors by adjusting the ICT character.[16–19] Lots of electron-donating π-building blocks have been used to tune the ICT; fluorenes,[16] carbazoles,[17] and so on. On the other hand, few numbers of electron-withdrawing counterparts that serve as general acceptor building blocks have been established except for naphthalene diimide, 2,1,3-benzothiadiazole, and *N*-containing heterocycles such as pyrazine and quinoxaline.[16,20–23]

In the present Letter, we report the synthesis and photoluminescent properties of novel fluorescent compounds based on a dipyrido[3,2-*a*:2′3′-*c*]phenazine (dppz) skeleton appended with electron-donating side-arms at its 10- and 13-positions, as shown in Figure 1. As dppz is an electron-deficient polycyclic compound, it should exhibit a strong electron-withdrawing character. In addition, the diimine site of dppz allows for coordination to various transition metal ions to yield stable metal–organic complexes with special electronic properties based on d-π perturbation. Indeed,

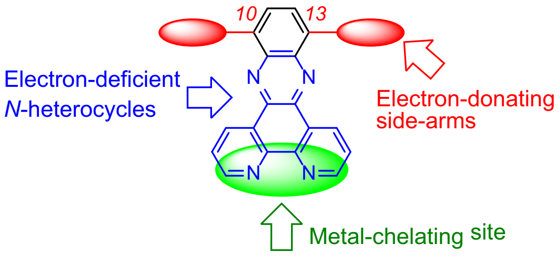

Figure 1. Molecular design of dppz-based ICT fluorophores.

---

[*] Corresponding author. Tel.: +81 72 254 9324; fax: +81 72 254 9910.
E-mail address: yagi@chem.osakafu-u.ac.jp (S. Yagi).

http://dx.doi.org/10.1016/j.tetlet.2014.07.069
0040-4039/© 2014 Elsevier Ltd. All rights reserved.

dppz derivatives have often been used as metallo-chelating ligands for DNA intercalators.[24,25] However, very few examples of dppz-based luminescent materials have been reported.[26] So we here demonstrate the development of novel highly emissive dppz-based fluorophores. We also report how the coordination of platinum(II) to the dppz fluorophore affected the emission properties through electronic perturbation in the ICT chromophoric system.

The synthesis of dppz derivatives **1a**–**g** and platinum(II) complexes **Pt**-**1e**–**g** is shown in Scheme 1. First, 4,7-dibromo-2,1,3-benzothiadiazole was converted to 4,7-disubstituted derivatives **2a**–**g** in excellent yields more than 80% except for **2c** (39%) by the Suzuki–Miyaura or the Sonogashira coupling reaction, followed by reduction with $LiAlH_4$ to obtain the diamines **3a**–**g** in 59–88% yields. The target compounds **1a**–**g** were prepared in 2–53% yields by condensation of **3a**–**g** with 1,10-phenanthroline-5,6-dione. The platinum(II) complexes **Pt**-**1e**–**g** were prepared by the reaction of **1e**–**g** with K_2PtCl_4 in 19–72% yields. The X-ray crystallographic analysis of the model compound of **Pt**-**1e** (i.e., **Pt**-**1e**′), that possesses 9,9-dimethylfluorenyl side-arms, revealed that platinum(II) coordinated to the diimine site of the dppz skeleton (Fig. 2).

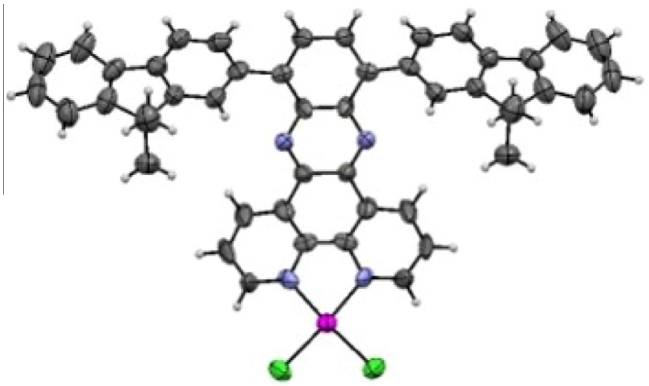

Figure 2. ORTEP view of the molecular structure for **Pt**-**1e**′ (See Supplementary data, Table S1 and Fig. S1).

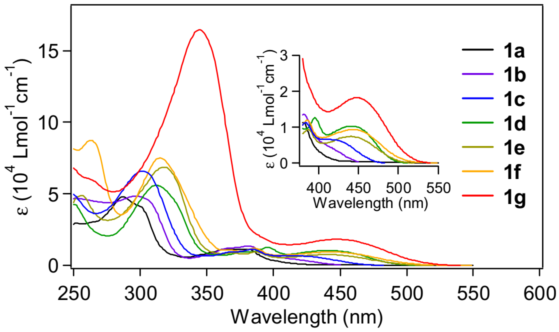

Figure 3. UV–vis absorption spectra (10 μM) of **1a**–**g** in dichloromethane at rt. Inset: enlarged view at 380–550 nm.

In Figure 3 are shown electronic absorption spectra of **1a**–**g** in dichloromethane at rt, and the spectral data are listed in Table 1. The dialkylated dppz **1a** exhibited absorption bands at 250–330 nm (molar absorption coefficient ε_{abs}; 47900 $M^{-1}\,cm^{-1}$ at 287 nm) and 330–450 nm (ε_{abs} = 12600 $M^{-1}\,cm^{-1}$ at 363 and 381 nm), assignable to π–π* and weak ICT transitions at the dppz chromophore, respectively. On the other hand, when the butyl groups were replaced by the phenyls (i.e., **1b**), the absorption shoulder emerged at 400–450 nm. Furthermore, when extensively π-conjugated aromatic components such as biphenylyl, phenylethynyl, fluorenyl, carbazolyl, and bifluorenyl groups were introduced at the 10- and 13-positions of dppz, broad absorption bands with relatively small ε_{abs} (6500–18200 $M^{-1}\,cm^{-1}$) were additionally observed for **1c**–**g** in the longer wavelength regions (400–530 nm), that are assignable to the transition bands based on the ICT from the electron donating side-arms to the dppz core. The assignment of the absorption bands to the ICT transitions was supported by TD-DFT calculations. In Figure 4 are shown the HOMO and LUMO profiles of **1e** and **1f**. The HOMO–LUMO transition of **1a** mainly occurs on dppz (See Supplementary data, Fig. S2), whereas, in the case of **1b**–**g**, the HOMO is delocalized on the π-conjugation system including both side-arms, and the LUMO is localized on the dppz moiety. These results clearly show that the attachment of electron-donating side-arms to dppz yielded D–A–D-type ICT chromophores, and thus the onset of the absorption spectrum was comparable to the electron-donating ability of the side-arms: a couple of side-arms as stronger donors gave a more bathochromically shifted onset, that is a narrower optical band gap E_g. The electrochemical properties, obtained by cyclic voltammetry (See Supplementary data, Fig. S3 and Table S2), clearly indicated that the reduction of E_g in accordance with the increase in the electron-donating ability was caused by both destabilization of HOMO and stabilization of LUMO.

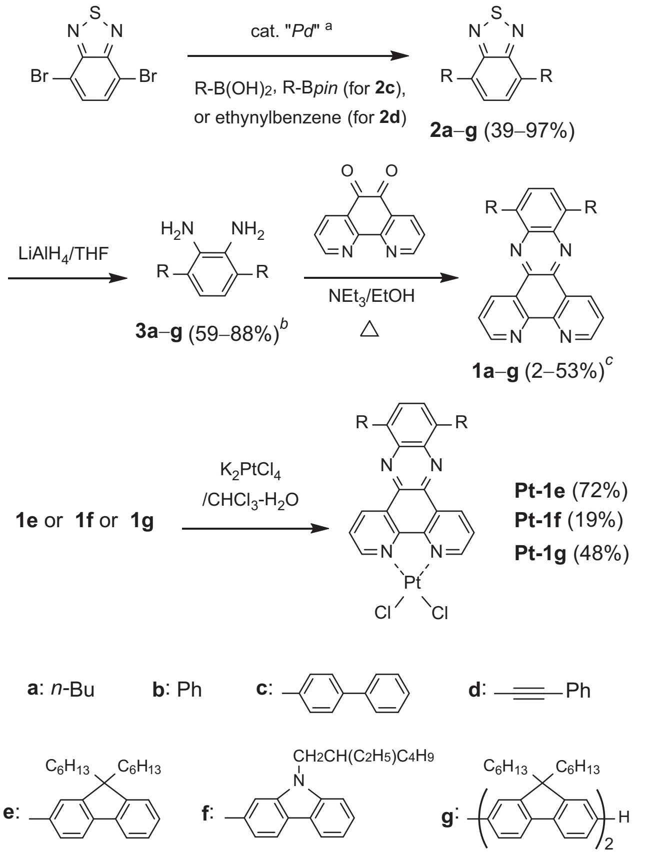

Scheme 1. Synthesis of **1a**–**g** and **Pt**-**1e**–**g**. [a]The detailed conditions are shown in Supplementary data. [b]As **3c** was poorly soluble, it was used in the next step without purification. So, the yield of **3c** was not obtained. [c]The yield of **1c** (2%) was determined as the one from **2c**.

Photoluminescence (PL) spectra of **1a**–**g** in dichloromethane at rt are shown in Figure 5, and the PL quantum yields (Φ_{PL}) and emission lifetimes (τ_{PL}) are also summarized in Table 1. Weak blue and bluish green emissions ($\Phi_{PL} \leqslant 0.10$) were observed for **1a** and **1b**, respectively, indicating that the dppz without strong donor side-arms is not so emissive. On the other hand, **1c**–**g** exhibited enhanced PL (Φ_{PL} = 0.49–0.91), the emission maxima λ_{PL} of which

Please cite this article in press as: Shigehiro, T.; et al. *Tetrahedron Lett.* (2014), http://dx.doi.org/10.1016/j.tetlet.2014.07.069

Table 1
UV–vis absorption (10 μM) and PL (1 μM) data of **1a–g** and **Pt-1e–g** in CH_2Cl_2 at rt

Compound	λ_{abs}/nm (ε_{abs}/L mol^{-1} cm^{-1})	E_g[a]/eV	λ_{PL} (λ_{ex})/nm	Φ_{PL}	τ_{PL}/ns (χ^2)
1a	287 (47900), 363 (12600), 381 (12600)	3.11	472 (301)	0.009	ND[b]
1b	297 (47900), 382 (13200)	2.73	505 (383)	0.10	1.79 (1.07)
1c	301 (66100), 384 (11200), 422 (6500)	2.63	522 (420)	0.68	11.2 (1.08)
1d	311 (56000), 395 (12600), 440 (10200)	2.52	522 (451)	0.91	11.5 (1.09)
1e	318 (69200), 387 (9300), 441 (7600)	2.48	569 (451)	0.84	13.7 (1.08)
1f	315 (75900), 386 (12000), 443 (9300)	2.45	579 (450)	0.49	9.34 (1.02)
1g	344 (166000), 448 (18200)	2.42	592 (452)	0.78	9.61 (1.00)
Pt-1e	318 (79400), 407 (11200), 475 (7800)	2.28	623 (450)	0.45	11.2 (1.00)
Pt-1f	314 (77600), 404 (12600), 475 (8300)	2.21	650 (469)	0.066	4.43 (1.06)
Pt-1g	346 (147900), 493 (11200)	2.20	655 (470)	0.24	5.57 (1.02)

[a] E_g values were estimated from the onset of UV–vis absorption spectra.
[b] Not determined due to too weak emission.

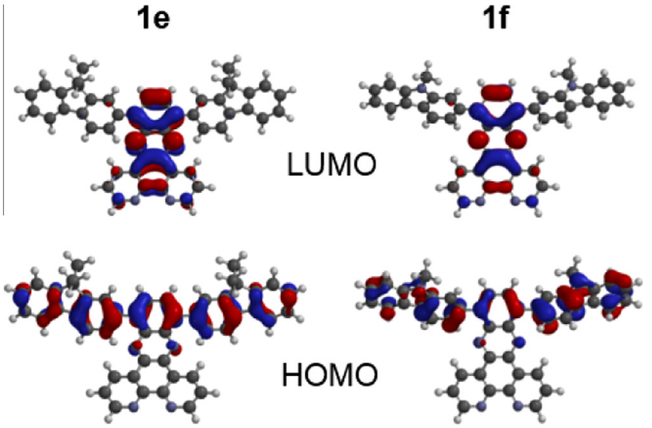

Figure 4. Electron distributions of the HOMO and LUMO for **1e** and **1f** calculated at the B3LYP/6-31G* level of theory (implemented in Gaussian 09 package[27]). The calculations were performed on the model structures in which the alkyl substituents are replaced by methyl groups.

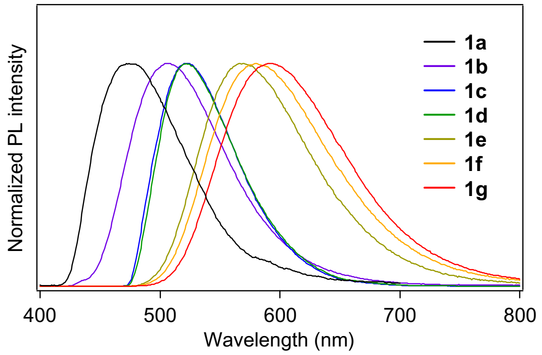

Figure 5. PL spectra (1 μM) of **1a–g** in CH_2Cl_2 at rt.

Table 2
PL data (1 μM) of **1e** in various solvents

Solvent (E_T(30))	λ_{PL} (nm)	Φ_{PL}	k_r (μs^{-1})	k_{nr} (μs^{-1})
Hexane (31.0)	524	0.74	79.2	27.8
Toluene (33.9)	538	0.99	104	1.05
Acetone (42.2)	572	0.99	68.3	0.690
DMSO (45.1)	590	0.99	72.8	0.735

range at 522–592 nm. The introduction of biphenylyl (**1c**) and phenylethynyl (**1d**) groups gave rise to green emission showing the λ_{PL}s at 522 nm. Upon comparison between **1c** and **1e**, suppressing the bond rotation of the biphenyl by the methano bridge led to a red shift of ca. 50 nm due to π-extension of the side-arms. As shown in **1g**, further extension of the side-arms by additional fluorenyl groups gave rise to a red shift at 592 nm, emitting strong orange PL (Φ_{PL} = 0.78). Hence, as is expected from the optical properties, the increase in electron-donating ability of the side-arms yielded red-shifted emission. It is worthy to note that the remarkable ICT is essential to obtain an enlarged Φ_{PL}.

ICT-based luminescence is often affected by solvent polarity.[30–32] So, the solvent effect on the emission behavior was investigated for the dppz-based chromophores. PL profiles of **1e–g** in various solvents are shown in Figure S4 and Table S3 (Supplementary data), and the data for **1e** are excerpted in Table 2 from Table S3. As the polarity of the solvent increased, positive solvatochromism of PL was observed for each of **1e–g**. For example, **1e** exhibited drastic PL spectral changes when the solvent polarity was varied: in hexane, **1e** exhibited green emission at 524 nm, whereas orange emission was observed at 590 nm in DMSO. On the other hand, the absorption spectra were almost unchanged (See Supplementary data, Fig. S4), indicating that these compounds are less polarized in the ground state. Thus, the positive solvatochromism observed for PL indicates that the present ICT-type chromophores are highly polarized in the excited states. Indeed, the differences in dipole moments between the excited states and the ground ones (Δμ) were investigated for **1e–g** by employing the Lippert–Mataga plot[28,29] (See Supplementary data, Fig. S5), and the Δμs for **1e–g** were estimated to be 12.3, 14.6, and 16.8 D, respectively. This result clearly shows that the increase in the electron-donating ability of the side-arms made the excited state more polarized. In terms of Φ_{PL}, a strong emission ($\Phi_{PL} \geqslant 0.74$) was observed for **1e**, regardless of solvent polarities. In general, the increase in solvent polarities made ICT-type chromophores less emissive because significant facilitation of nonradiative decay was caused by solvent relaxation.[30,31] For **1e**, however, the increase in the nonradiative decay rate k_{nr} was suppressed even in highly polar solvents such as acetone and DMSO (Table 2). Thus, **1e** was still highly emissive in these solvents (Φ_{PL} = 0.99). The excellent luminescent properties of **1e** make itself potentially applicable to a fluorescent probe in polar media.[32] In the case of **1f**, the nonradiative decay was facilitated with the increase in solvent polarity, as shown in Table S3. Taking the Δμ value of **1f** into consideration, one can see that the deteriorated PL of **1f** in polar solvents is attributed to the more polarized excited state in comparison with that of **1e**. Thus, **1f** should be susceptible to emission quenching by solvent relaxation. On the other hand, **1g** exhibited relatively intense emission even in polar solvents despite the large Δμ value. Although the detailed mechanism is still unclear, we found that the fluorene-derived side-arms are effective to obtain highly emissive dppz derivatives in wide range of solvents.

Taking advantage of metal-chelation ability of the diimine site, the platinum(II) complexes **Pt-1e–g** were also prepared. These

Please cite this article in press as: Shigehiro, T.; et al. *Tetrahedron Lett.* (2014), http://dx.doi.org/10.1016/j.tetlet.2014.07.069

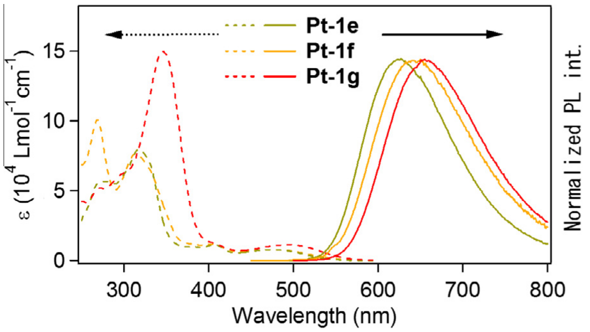

Figure 6. UV–vis absorption (10 μM) and PL (1 μM) spectra of **Pt-1e–g** in dichloromethane.

complexes exhibited the solubility of 0.91–100 mg/mL in dichloromethane, although platinum(II) complexes often exhibit low solubility in organic solvents due to strong stacking interactions. The UV–vis absorption and PL spectra are depicted in Figure 6, and the spectral data are summarized in Table 1. In the absorption spectra, broadened bands assignable to the ICT transitions were observed at 400–600 nm for **Pt-1e–g**, which are red-shifted by 32–45 nm in comparison with the ICT bands of the corresponding ligands **1e–g**. In PL spectra, **Pt-1e–g** exhibited red emission (λ_{PL} = 623–655 nm), the lifetimes of which are on the order of nanoseconds (τ_{PL} = 4.43–11.2 ns). The relatively short τ_{PL}s indicate that the present platinum(II) complexes crucially emit fluorescence, in spite of the fact that phosphorescent platinum(II) complexes are widely known due to their potential as emitting dopants for phosphorescent OLEDs.[33,34] Taking the bathochromic shift of the ICT transition band in each platinum(II) complex into consideration, the red-shifted emission is attributed to the facilitation of the ICT by the coordination of the Lewis acidic platinum(II) ion. In terms of electrochemical properties (See Supplementary data, Table S2), the platinum(II) coordination made the reduction potential shifted in a positive direction in comparison with that of the corresponding ligand, and thus the LUMO was more stabilized.[35]

In summary, we developed a series of luminescent dppz derivatives, although dppz is not emissive. The D–A–D structure causing the strong ICT transition is essential to yield excellent PL properties. The PL properties are tuned by controlling the ICT character, that is varying the donor components, and thus a wide range of emission colors have been achieved from blue (**1a**) to orange (**1g**). We also obtained the platinum(II) complexes of some dppz derivatives. They exhibit more red-shifted fluorescence in comparison with the corresponding ligands, showing their λ_{PL} in the red region (λ_{PL} = 623–655 nm). This significant red shift is due to the facilitation of the ICT by the coordination of a platinum(II) ion working as a Lewis acid.

Acknowledgements

This work was supported by a Grants-in-Aid for Scientific Research on Innovative Areas ‘New Polymeric Materials Based on Element-Blocks (No. 2401)’ (25102537) of The Ministry of Education, Culture, Sports, Science, and Technology, Japan.

Supplementary data

Supplementary data (synthetic procedures, characterization data including crystal structure analysis of **Pt-1e′**, results of DFT calculations, electrochemical data, and optical and PL data in various solvents) associated with this article can be found, in the online version, at http://dx.doi.org/10.1016/j.tetlet.2014.07.069. The supplementary crystallographic data for **Pt-1e′** have been deposited with the Cambridge Crystallographic Data Centre as supplementary publications CCDC 1007550. Copies of the data can be obtained free of charge by application to CCDC, 12 Union Road, Cambridge CB21EZ, UK (e-mail: deposit@ccdc.cam.ac.uk).

References and notes

1. Zhang, X.; Ren, X.; Xu, Q.-H.; Loh, K. P.; Chen, Z.-K. *Org. Lett.* **2009**, *11*, 1257–1260.
2. Suzuki, Y.; Yokoyama, K. *J. Am. Chem. Soc.* **2005**, *127*, 17799–17802.
3. Samuel, W.; Thomas, III; Joly, G. D.; Swager, T. M. *Chem. Rev.* **2007**, *107*, 1339–1386.
4. Witulski, B.; Weber, M.; Bergsträsser, U.; Desvergne, J.-P.; Bassani, D. M.; Bouas, L. H. *Org. Lett.* **2001**, *3*, 1467–1470.
5. Ajayaghosh, A.; Carol, P.; Sreejith, S. *J. Am. Chem. Soc.* **2005**, *127*, 14962–14963.
6. Coskun, A.; Deniz, E.; Akkaya, E. U. *Org. Lett.* **2005**, *7*, 5187–5189.
7. Kulkarni, A. P.; Kong, X.; Jenekhe, S. A. *Adv. Funct. Mater.* **2006**, *16*, 1057–1066.
8. Zhang, M.; Xue, S.; Dong, W.; Wang, Q.; Fei, T.; Gu, C.; Ma, Y. *Chem. Commun.* **2010**, *46*, 3923–3925.
9. Jones, G., II; Jackson, W. R.; Choi, C.-Y. *J. Phys. Chem.* **1985**, *89*, 294–300.
10. Kubin, R. F.; Fletcher, A. N. *J. Lumin.* **1982**, *27*, 455–462.
11. Sims, P. J.; Waggoner, A. S.; Wang, C.-H.; Hoffman, J. F. *Biochemistry* **1974**, *13*, 3315–3330.
12. Kalyanasundaram, K.; Thomas, J. K. *J. Am. Chem. Soc.* **1977**, *99*, 2039–2044.
13. Thomas, S. W., III; Yagi, S.; Swager, T. M. *J. Mater. Chem.* **2005**, *15*, 2829–2835.
14. Gettinger, C. L.; Heeger, A. J.; Drake, J. M.; Pine, D. *J. Chem. Phys.* **1994**, *101*, 1673–1678.
15. Hirohata, M.; Tada, K.; Kawai, T.; Onoda, M.; Yoshino, K. *Synth. Met.* **1997**, *85*, 1273–1274.
16. Karpicz, R.; Puzinas, S.; Krotkus, S.; Kazlauskas, K.; Jursenas, S.; Grazulevicius, J. V.; Grigalevicius, S.; Gulbinas, V. *J. Chem. Phys.* **2011**, *134*. 204508-1–9.
17. Moss, K. C.; Bourdakos, K. N.; Bhalla, V.; Kametekar, K. T.; Bryce, M. R.; Fox, M. A.; Vaughan, H. L.; Dias, F. B.; Monkman, A. P. *J. Org. Chem.* **2010**, *75*, 6771–6781.
18. Tanaka, H.; Shizu, K.; Nakanotani, H.; Adachi, C. *Chem. Mater.* **2013**, *25*, 3766–3771.
19. Wang, K.; Huang, S.; Zhang, Y.; Zhao, S.; Zhang, H.; Wang, Y. *Chem. Sci.* **2013**, *4*, 3288–3293.
20. Achelle, L.; Baudequin, C.; Plè, N. *Dyes Pigments* **2013**, *98*, 575–600.
21. Hancock, J. M.; Gifford, A. P.; Zhu, Y.; Lou, Y.; Jenekhe, S. A. *Chem. Mater.* **2006**, *18*, 4924–4932.
22. Kim, Y.; Hong, J.; Oh, J. H.; Yang, C. *Chem. Mater.* **2013**, *25*, 3251–3259.
23. Li, H.; Kim, F. S.; Ren, G.; Hollenbeck, E. C.; Subramaniyan, S.; Jenekhe, S. A. *Angew. Chem., Int. Ed.* **2013**, *52*, 5513–5517.
24. McKinley, A. W.; Lincoln, P.; Tuite, E. M. *Coord. Chem. Rev.* **2011**, *255*, 2676–2692.
25. Li, M.; Lincoln, P.; Andersson, J. *J. Phys. Chem. B* **2011**, *115*, 7923–7931.
26. Choi, C.-S.; Jeon, K.-S.; Lee, K.-H.; Yoon, M.; Kwak, M.; Lee, S. W.; Kim, I. T. *Bull. Korean Chem. Soc.* **2006**, *27*, 1601–1603.
27. Frisch, M. J. et al. *Gaussian 09*, Revision A. l; Gaussian Inc: Wallingford, CT, 2009 (the complete description for this reference is provided in the Supplementary data).
28. Lippert, V. E. *Z. Elektrochem.* **1957**, *61*, 962–975.
29. Mataga, N.; Kaifu, Y.; Koizumi, M. *Bull. Chem. Soc. Jpn.* **1956**, *29*, 465–470.
30. Otsuka, K.; Kondo, T.; Nishiyabu, R.; Kubo, Y. *J. Org. Chem.* **2013**, *78*, 5782–5787.
31. Kubota, Y.; Ozaki, Y.; Funabiki, K.; Matsui, M. *J. Org. Chem.* **2013**, *78*, 7058–7067.
32. Tainaka, K.; Tanaka, K.; Ikeda, S.; Nishiza, K.; Unzai, T.; Fujiwara, Y.; Saito, I.; Okamoto, A. *J. Am. Chem. Soc.* **2007**, *129*, 4776–4784.
33. Brooks, J.; Babayan, Y.; Lamansky, S.; Djurovich, P. I.; Tsyba, I.; Bau, R.; Thompson, M. E. *Inorg. Chem.* **2002**, *41*, 3055–3066.
34. Williams, J. A. G.; Beeby, A.; Davies, E. S.; Weinstein, J. A.; Wilson, C. *Inorg. Chem.* **2003**, *42*, 8609–8611.
35. Welch, G. C.; Bazan, G. C. *J. Am. Chem. Soc.* **2011**, *133*, 4632–4644.